RESEARCH ARTICLE | MAY 24 2024

Phonon-mediated quantum efficiency measurement in semiconductors

W. Baker ; N. Mirabolfathi

Appl. Phys. Lett. 124, 212105 (2024)
https://doi.org/10.1063/5.0203833

Applied Physics Letters ARTICLE pubs.aip.org/aip/apl

Phonon-mediated quantum efficiency measurement in semiconductors

Cite as: Appl. Phys. Lett. **124**, 212105 (2024); doi: 10.1063/5.0203833
Submitted: 16 February 2024 · Accepted: 9 May 2024 ·
Published Online: 24 May 2024

W. Baker[a] and N. Mirabolfathi

AFFILIATIONS

Department of Physics and Astronomy, Texas A&M University, College Station, Texas 77843, USA

[a]Author to whom correspondence should be addressed: williambaker@tamu.edu

ABSTRACT

Accurate quantum efficiency measurement not only provides crucial information for the photovoltaic cell industry but also supports experiments aimed at directly detecting dark matter and elastic neutrino interactions. The dark matter direct searches paradigm has recently expanded to include particles with masses below $1\,\mathrm{MeV}/c^2$, where the expected signal in an electron–recoil interaction is approximately in the eV range, just above the energy gap for silicon and germanium. A robust calibration method for ionization signals in this lower energy region is essential. This paper presents a method for measuring quantum efficiency and yield (q/E) in semiconductors using phonon-mediated calorimetry. The Neganov–Trofimov–Luke phonon amplification method in low-temperature semiconductor crystals has been employed to indirectly measure ionization down to single-electron accuracy. Specifically, at zero bias, the phonon readout directly quantifies the total energy deposited within the detector, independent of the ionization yield. This eliminates a significant source of systematic uncertainty in quantum efficiency estimates associated with total energy uncertainty. The paper includes results from an updated ionization efficiency measurement in a germanium detector.

The search paradigm for dark matter direct detection is expanding to encompass particles with masses well below the GeV/c^2 scale.[1] At this level, the contribution of interactions between dark matter and electrons becomes significantly important compared to the interactions between dark matter and nuclei. In experiments utilizing semiconductor ionization detectors, the calibration of ionization efficiency for electron recoil events becomes crucial, especially as the interaction energy approaches the semiconductor gap. Data from these searches are typically compared and calibrated against well-studied high-energy sources, where the ionization yield—the number of charge pairs released per input energy—is well documented.[2–7] For an accurate and reliable analysis of the incident particle's nature, it is imperative to include an accurate estimation of the quantity of charge produced in the interaction. In particular, the ionization efficiency at energies close to the semiconductor gap varies significantly compared to high-energy interactions.

To date, the measure of ionization efficiency in silicon and germanium has primarily relied on experiments utilizing the statistical estimation proposed by Shockley.[8] This mean value of energy per charge pair in silicon (3.6 eV) or germanium (2.98 eV) was predicted by Shockley and subsequently measured by several groups.[2–7,9] The method for determining these values is relatively straightforward, involving a known light source, a target sample (Si, Ge, etc.), and a secondary, calibrated detector to collect light reflected off the sample. Knowledge of the incident energy, the intensity, and current in the secondary detector enables a simple calculation to determine the absorbed energy, and measuring the current through the sample is used to quantify the ionization efficiency.

This method is burdened with systematic uncertainties, with the primary concern being the determination of the absorbed energy by the detector. Current estimates heavily rely on models and primarily hinge on reflectivity measurements, which are essential for accurately assessing absorbed energy. Sample reflectivity, a variable quantity in the visible range, is highly dependent on surface roughness, treatment, and the specifics of the interface at which light interacts with the sample. In the case of germanium, different contemporary publications have reported reflectivities differing by a factor of two, resulting in significantly varied estimations of ionization efficiency. Setting aside the challenge of controlling systematics, this measurement inherently involves three distinct components: a measurement of sample current, a measurement of reflectivity, and a measurement of unabsorbed light via secondary detector current. The last two measurements are necessary to calibrate the first measurement because the energy absorbed by the sample is unknown, introducing uncontrollable systematic uncertainties.

A measurement method exists that offers a straightforward, singular, and independent assessment of efficiency in semiconductors. Ionization signals fundamentally entail observing drifting charges. However, as drifting carriers scatter off the lattice, they generate high-energy phonons, and the intensity of these phonons is proportional to the number of carriers. This implies that phonon signals can measure ionization under biased conditions and estimate the total absorbed energy under unbiased conditions. This approach mitigates a significant systematic error in measuring ionization efficiency.

Our phonon-mediated ionization measurement is based on the Neganov–Trofimov–Luke (NTL) effect. The transport of charge through a semiconductor generates phonons whose total energy E_{NTL} is equal to the liberated electric potential energy, and thus is proportional to both the bias voltage applied across the detector V_{ext} and the number of charges N,

$$E_{NTL} = N \cdot e \cdot V_{ext}. \tag{1}$$

The number of charges produced in the interaction in turn is proportional to the energy deposited in the interaction E_0 and the ionization efficiency ε, which we will use with units of energy per pair created (N),

$$N = \frac{E_0}{\varepsilon}. \tag{2}$$

Assuming that charge is not lost or gained from trapping/detrapping or recombination, the total energy $E_0 + E_{NTL}$ is simply

$$E_{Total} = E_0\left(1 + \frac{e \cdot V}{\varepsilon}\right). \tag{3}$$

We will assume for the sake of this measurement that at large enough fields, the effects of recombination and trapping are not a significant contributor. If it were, one should add a bias-dependent term to this model.

Conventional semiconductor ionization rate measurements rely on charge transport and readout using high impedance front-end charge amplifiers, constrained by large detector capacitance and sensitivity limitations. Low-threshold phonon-mediated detectors offer superior sensitivity. In the absence of significant leakage current or breakdown, both phonon signal amplitude and the signal-to-noise ratio (S/N) increase linearly with bias voltage. Paul Luke[10] demonstrated years ago that these phonon measurements can be a highly sensitive indirect measure of ionization through Neganov–Trofimov–Luke amplification. CDMS, employing NTL technology, achieved unprecedented resolution (< 0.1 eV$_{ee}$) (Ref. 11) in small mass silicon detectors, with a modest exposure of $\sim$0.5 g day in a ground-level facility, setting limits for DM–matter interactions.[12,13] The EDELWEISS experiment also uses this technology for low-resolution measurements.[14]

Our detectors, similarly to CDMSlite,[15] deploy very low noise transition edge sensor (TES) phonon readouts[16] to indirectly measure ionization using the Neganov–Trofimov–Luke effect in very low-temperature semiconductor absorbers.

To maximize phonon collection efficiency, our standard detector phonon sensors cover the majority of the detector surface. However, this extensive coverage by metallic surfaces introduces a systematic issue for our photon detection. Specifically, the photons absorbed by the metallic films generate phonons without electron–hole pairs, resulting in an apparent lower ionization yield. In a previous study, to mitigate leakage current in our low-threshold high-voltage detectors, our group developed a contact-free geometry. This involved introducing a vacuum gap between the bias electrode and the substrate, leaving one surface of the detector polished and without contacts.[17,18] This biasing technique enables direct exposure of the semiconductor to photons. The detector used in this work employs a similar contact-free technique.

To date, the NTL effect has been employed to retroactively determine the initial signal strength of an interaction, enabling phonon-mediated measurements of small ionization signals. We have reversed this calculation to perform the measurement of efficiency, leveraging information about both the original and amplified signals. Assuming a linear proportionality between signal amplitude and energy, Eq. (3) can be expressed as

$$A_{Total} = A_0\left(1 + \frac{e \cdot V}{\varepsilon}\right). \tag{4}$$

Therefore, measuring ε involves simply determining the slope and the intercept on a plot of amplitude vs bias,

$$\varepsilon = \frac{b}{m}. \tag{5}$$

In this context, the intercept signifies the interaction energy in arbitrary units. The slope represents the signal or energy gain from NTL amplification, measured in units of inverse energy. Consequently, the quantum efficiency can be determined without a prior assumption about the total energy.

Our test device to demonstrate this method consists of a small, coin-sized crystal patterned on one face with CDMS-style Transition Edge Sensors, and the reverse face polished smooth and bare. A block diagram along with sensor layout and design is visible in Fig. 1. As mentioned earlier, a vacuum electrode on the bare face provides the biasing field, generating NTL gain, while the phonon sensors are biased and read out through SQUID current amplifiers. Average pulses at various biases along with their associated noise spectra are in Fig. 2. A small hole in the vacuum electrode allows a mounted fiber optic to project controlled light pulses onto the bare surface, and both an ^{241}Am and ^{55}Fe source are mounted, exposed to the patterned face. Although this measurement does not inherently require energy calibration, including these sources is necessary due to the vacuum gap impeding direct knowledge of the electric potential across the semiconductor. Manually pulsed laser light is provided by nanosecond pulsed laser (NPL series) diodes from ThorLabs emitting at 450 (2.75 eV), 640 (1.94 eV), and 980 nm (1.27 eV) and guided through optical fibers from room temperature to the cold volume of the refrigerator. The detector bias was varied from 0 to $\sim$20 V, and the resultant pulse height is recorded for laser photons and 6 keV from ^{55}Fe.

We calibrate the vacuum gap thickness by measuring the gain in signal vs bias for the ^{55}Fe source 6 keV photons. Determining the slope and intercept for these events yields an apparent efficiency of nearly 4.6 eV/pair. Setting the potential drop across the vacuum using the well-studied efficiency for high-energy events in Ge (2.98 eV/pair),[2] we can calibrate the gap via

$$d_{\text{gap}} = \left(d_{\text{crystal}}\left[\frac{1}{\kappa} - 1\right]\right)\varepsilon_R^{-1}, \tag{6}$$

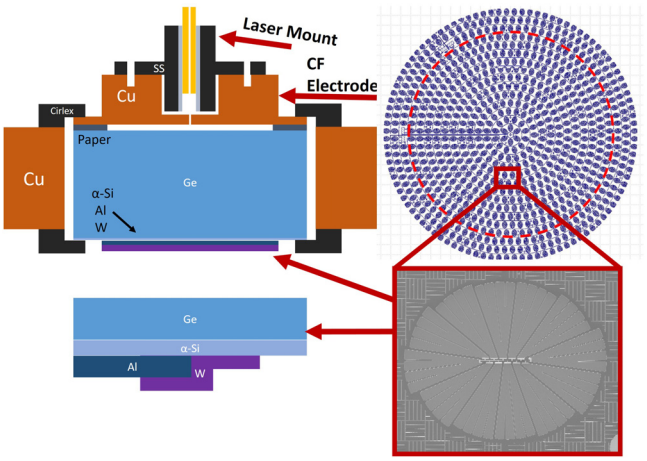

FIG. 1. Germanium "coin" detector, measuring 25 mm ∅ by 7 mm thick. Paper ≈300 um thick is used to insulate the crystal from the copper contact-free (CF) electrode. The electrode also accommodates a stainless steel (SS) mount for the laser filament and is secured to the detector via Cirlex clamps. The reverse side of the detector is lithographically patterned with an array of tungsten transition edge sensors with aluminum fins for high energy phonon collection, and a thin layer of amorphous silicon (α-Si). This surface is also insulated from chassis by Cirlex clamps. The image in the top right is the sensor arrangement on the patterned surface with an SEM scan of a single sensor below it and the cross sectional diagram of the sensor on the bottom left. The thin line at the center is the tungsten film, overlaying the aluminum fins, which comprise the bulk of the sensor.

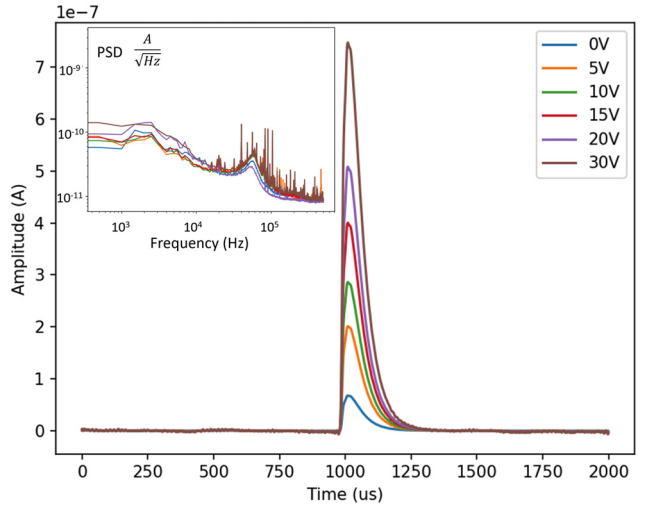

FIG. 2. Average pulses from laser light tuned to have energy equivalent of 1.5 keV with linearly increasing amplitude vs applied bias up to 30 V, while the noise power spectral density shows only a slight increase (inset).

where d_X are the thicknesses of the gap and crystal, κ is the dielectric of germanium (15.8), and ε_R is the vacuum permittivity. For this device, we estimated the gap to be 340 μm, which is very close to the expected gap from our paper spacer. We can use this same process to correct the actual potential across the semiconductor sample as a function of the applied potential through a simple scale factor. It should be noted that the uncertainty introduced through this calibration is relatively small compared to the measurement itself considering it is extracted from a linear fit over many points, but is still propagated appropriately.

The initial validation of this method was conducted with the 640 nm laser. The stability and linearity of the detector were assessed before biasing (Fig. 3—left). The 60 and 6 keV photons from ^{241}Am and ^{55}Fe, as well as the lower-energy events from the ^{241}Am source, are observable. Energy linearity is affirmed by the relative sizes of the 6 and 60 keV events. It should be noted that the 60 keV events are generally too large for this particular detector, resulting in saturated pulses and as such these events are not used for any analysis presented here. The particulars of how pulse amplitudes are calculated depend on a method of template fitting, which does not take into account saturation effects that lead to a spectrum broadening at higher energies. Biasing between 0 and 20 V and measuring the pulse heights of each event allow us to use the 0 V pulse height as our intercept. Each subsequent pulse height is then collected, and the difference between these two values represents the gain at that bias. Cross-calibrating the 6 and 60 keV events with this method provides the same quantum efficiency at 3 eV/pair.

The absence of metallic contact at the bare surface of our detector results in a progressive charge buildup on that surface. This accumulated charge generates a counter electric field, leading to a smaller NTL gain, as depicted in Fig. 3 (right).

Without significant leakage current, this effect is anticipated to rely solely on the event rate, as charge pairs are created and drifted. Indeed, a linear behavior in pulse height vs time is observed, as depicted in the right part of Fig. 3. The pulse height relevant to this measurement is the uncompensated pulse height, or the amplitude at the moment of bias. This can be easily extracted by fitting the initial portion of each dataset, which is linear and using the t = 0 intercept. Initially, we conducted these calculations using a red laser and observed the expected linear response of gain vs bias.

The second check involves ensuring consistency. Laser pulses are much shorter (∼10 ns) than the phonon collection time in our sensors (∼μs) and so pulse width is effectively translated directly to packet energy. By manually adjusting the energy of each pulse during laser pulsing, we confirm the linearity of the measurement. If the ionization efficiency depends on the energy of individual photons rather than the total event energy of the pulse, altering the pulse width and amplitude should not affect our measurement.

Finally, we vary the photon energy using lasers of different wavelengths (Fig. 4). Measurements with blue (450 nm), red (640 nm), and near-IR (980 nm) lasers have produced comparable results above 2.5 eV, with slight deviations as laser energies approach the gap energy in Ge. It is crucial to distinguish between yield and efficiency, as they are related quantities. Our direct measurement focuses on efficiency—the energy cost per charge pair created in an interaction. Yield is essentially the inverse, representing the number of charge pairs per input energy. At energies slightly above the gap, yield should be approximately 1, as reported in older publications. For energies just above the gap, there exists an inverse relationship between yield and efficiency. The numbers recorded in Fig. 4 display both efficiency and yield to facilitate a more direct comparison with previous measurements.

We measure the gain for every bias starting from 0. However, the only data points relevant for quantum efficiency measurement are the

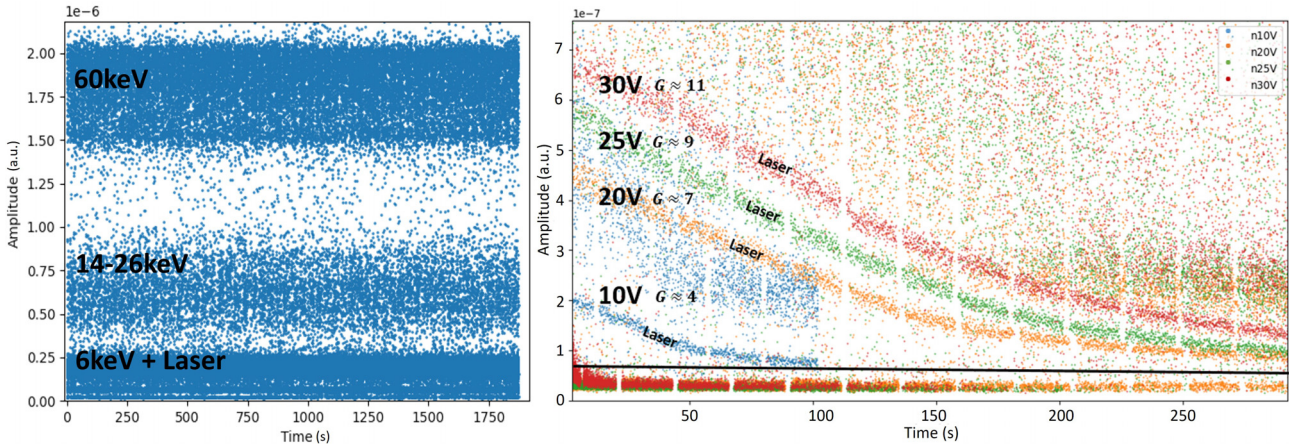

FIG. 3. Left: Amplitude vs detector run time with 0 detector bias, before data quality cuts are applied. Right: 640 nm laser pulse height vs time for various external biases without gap correction. Contact-free geometries result in a charging effect, which effectively screens the internal field of a detector. The pulse height used for calculation is the pulse height at the moment of bias. This number is extracted by applying a linear fit to the pulse height vs time plot and calculating the intercept. The solid black line at the bottom indicates the zero-bias level of the laser amplitude. Vertical gaps in data correspond to down time required to save buffered data.

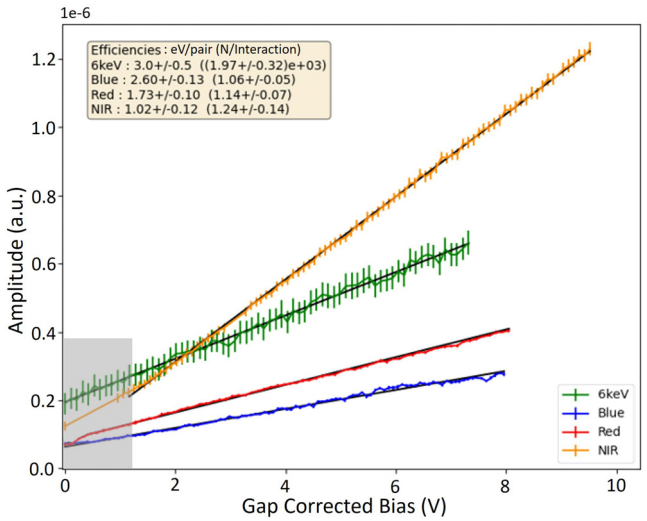

FIG. 4. 6 keV pulse heights alongside blue (450 nm - 2.76 eV), red (640 nm - 1.97 eV), and near-IR (980 nm - 1.27 eV) laser pulse heights as a function of corrected detector bias. Each laser energy was measured in separate experiments. The slope divided by the intercept (ionization efficiency) of each dataset is recorded in the top left with the yield (event energy/efficiency) adjacent. Note that the intercept used in this calculation is the measurement made at 0 bias, and not the intercept of the fit. Collection issues and short datasets result in "flat" regions at low bias, which are not accounted for in this model. Also note that each dataset is collected in a separate run, meaning that the specifics of detector condition, such as temperature, can vary slightly.

amplitude at 0 V and the slope at higher voltages. Independently of the quantum efficiency, the ionization collection at low biases can be affected by physical processes such as recombination and trapping. Thus, we exclude that segment of the data from our analysis. Low bias data are highlighted in gray in Fig. 4 to illustrate the range of data that is excluded from fitting. Identical measurements were performed using a negative bias with similar analysis parameters, yielding the same results.

As summarized in Table I, there are marginal differences between the results of the measurement presented here and historical measurements, particularly deviating at lower energies. It is evident that historical measurements were not in complete agreement about the efficiency as photon energy approached the gap energy, but our measurement consistently yields smaller efficiency for lower photon energies. Our primary systematic concern is the vacuum gap, which we have accounted for. A subsequent measurement is already planned, implementing a patterned grid on the face that currently has the gap. This will enable a calibration-less measurement of efficiency and eliminate the gap estimation as a necessary step. Recombination of carriers at the surfaces could also contribute to discrepancies at lower biases, as charges reaching the unpatterned surface may not necessarily relax their energy back to the crystal—a grid patterning resolves this issue as well.

Discrepancies between the numbers reported here and those from previous studies, especially at low energy efficiency, likely stem from the specific systematics in how earlier publications accounted for the energy absorbed by their samples. It is entirely conceivable that previous studies may have overestimated the energy absorbed by their samples, leading to higher estimations of energy/pair. The measurement presented here, in contrast, does not rely on precise accounting of the absorbed energy, making it less susceptible to such uncertainties.

We have demonstrated a robust, updated method of measuring quantum efficiency in semiconductors, which benefits from low noise low-temperature phonon readout. The method alleviates the main challenge of the previous measurements, i.e., the estimate of the total absorbed energy in the detector. This is an important step toward determining the nature of low energy electron recoil events in the field of rare-particle searches and in understanding the exact mechanism of ionization excitation in the broader field of semiconductor science. Our first measurement of ionization efficiency using this method revealed discrepancies with the values previously reported that are likely due to the difference in the systematics associated with different

TABLE I. Ionization efficiency in eV/pair in germanium as reported by various authors. Values are approximated for works in which data are not numerically recorded. Note that the value we report for energies above 3 eV (i.e., 6 and 60 keV) is a value, which is fixed due to the requirement of gap calibration in our particular setup. Using a value of 2.8 or 2.9, for example, would shift the reported values for each other wavelength accordingly.

Energy (eV):	1.27 (Near-IR)	1.97 (Red)	2.76 (Blue)	>3.00
This work	1.02 ± 0.12	1.73 ± 0.1	2.6 ± 0.13	3.0
Vavilov[4]	1.27	1.97	2.76	3.7
Christenson[7]	1.22	1.89	2.6	2.83
Tauc[3]	1.34	2.07	2.51	2.9
Koc[9]	1.27	1.97	2.51	2.5
Klein[5]	N/A	N/A	N/A	2.8
Antman[6]	N/A	N/A	N/A	2.98
McKay[2]	N/A	N/A	N/A	2.9

measurement methods. We plan on repeating this measurement on silicon and other common semiconductors using phonon-mediated detector with different contact architectures.

This work was supported by the Department of Energy (DOE, USA) Grant de-sc0018981 as well as the National Science Foundation (NSF) Grant NSF OISE 1743790.

The authors also express thanks to Mr. Mark Platt and Dr. Rupak Mahapatra for fabricating the Ge detector used in this study. Additionally, Ms. Chelsea Savage's assistance played a crucial role in building the experimental setup.

AUTHOR DECLARATIONS

Conflict of Interest

The authors have no conflicts to disclose.

Author Contributions

William Baker: Conceptualization (equal); Data curation (lead); Formal analysis (lead); Investigation (equal); Methodology (equal); Software (lead); Writing – original draft (lead); Writing – review & editing (equal). **Nader Mirabolfathi:** Conceptualization (equal); Funding acquisition (lead); Methodology (equal); Project administration (lead); Supervision (equal); Writing – review & editing (equal).

DATA AVAILABILITY

The data that support the findings in this study are available from the corresponding author upon request.

REFERENCES

[1]S. Cebrián, "Review on dark matter searches," J. Phys.: Conf. Ser. **2502**, 012004 (2023).
[2]K. G. McKay and K. B. McAfee, "Electron multiplication in silicon and germanium," Phys. Rev. **91**, 1079–1084 (1953).
[3]J. Tauc, "Electron impact ionization in semiconductors," J. Phys. Chem. Solids **8**, 219–223 (1959).
[4]V. S. Vavilov, "On photo-ionization by fast electrons in germanium and silicon," J. Phys. Chem. Solids **8**, 223–226 (1959).
[5]S. Antman, D. Landis, and R. Pehl, "Measurements of the Fano factor and the energy per hole-electron pair in germanium," Nucl. Instrum. Methods **40**, 272–276 (1966).
[6]C. Klein, "Simple explanation of the electron-hole pair creation energy puzzle in germanium," Phys. Lett. A **24**, 513–514 (1967).
[7]O. Christensen, "Quantum efficiency of the internal photoelectric effect in silicon and germanium," J. Appl. Phys. **47**, 689–695 (1976).
[8]W. Shockley, "Problems related top-*n* junctions in silicon," Czech. J. Phys. **11**, 81–121 (1961).
[9]S. Koc, "The quantum efficiency of the photo-electric effect in germanium for the 0.3–2 wavelength region," Czech. J. Phys. **7**, 91–95 (1957).
[10]P. Luke, J. Beeman, F. Goulding *et al.*, "Calorimetric ionization detector," Nucl. Instrum. Methods Phys. Res. Sect. A **289**, 406–409 (1990).
[11]R. Romani, P. Brink, B. Cabrera *et al.*, "Thermal detection of single e-h pairs in a biased silicon crystal detector," Appl. Phys. Lett. **112**, 043501 (2018).
[12]R. Agnese, T. Aralis, T. Aramaki *et al.*, "First dark matter constraints from a superCDMS single-charge sensitive detector," Phys. Rev. Lett. **121**, 051301 (2018).
[13]D. W. P. Amaral, T. Aralis, T. Aramaki *et al.*, "Constraints on low-mass, relic dark matter candidates from a surface-operated superCDMS single-charge sensitive detector," Phys. Rev. D **102**, 091101 (2020).
[14]H. Lattaud, E. Armengaud, Q. Arnaud *et al.*, "Sub-MeV dark matter searches with EDELWEISS: Results and prospects," arXiv:2211.04176 (2022).
[15]R. Agnese, A. J. Anderson, M. Asai *et al.*, "Search for low-mass weakly interacting massive particles using voltage-assisted calorimetric ionization detection in the SuperCDMS experiment," Phys. Rev. Lett. **112**, 041302 (2014).
[16]K. D. Irwin, "Phonon-mediated particle detection using superconducting tungsten transition-edge sensors," Ph.D. thesis (Stanford University, 1995).
[17]N. Mirabolfathi, H. R. Harris, R. Mahapatra *et al.*, "Toward single electron resolution phonon mediated ionization detectors," Nucl. Instrum. Methods Phys. Res. Sect. A **855**, 88–91 (2017).
[18]V. Iyer, N. Mirabolfathi, G. Agnolet *et al.*, "Large mass single electron resolution detector for dark matter and neutrino elastic interaction searches," Nucl. Instrum. Methods Phys. Res. Sect. A **1010**, 165489 (2021).